THE CHARACTER OF LOW-LYING EXCITED STATES OF MIXED-LIGAND METAL CARBONYLS. TD-DFT AND CASSCF/CASPT2 STUDY OF $[W(CO)_4L]$ (L = ETHYLENEDIAMINE, *N,N′*-DIALKYL-1,4-DIAZABUTADIENE) AND $[W(CO)_5L]$ (L = PYRIDINE, 4-CYANOPYRIDINE)

Stanislav ZÁLIŠ[a1,*], Antonín VLČEK, Jr.[a,b] and Chantal DANIEL[c]

[a] *J. Heyrovský Institute of Physical Chemistry, Academy of Sciences of the Czech Republic, Dolejškova 3, CZ-182 23 Prague, Czech Republic; e-mail:* [1] *zalis@jh-inst.cas.cz*

[b] *Department of Chemistry, Queen Mary, University of London, Mile End Road, London E1 4NS, United Kingdom; e-mail: a.vlcek@qmul.ac.uk*

[c] *Laboratoire de Chimie Quantique, UMR 7551 CNRS/Université Louis Pasteur, Institut Le Bel, 4 Rue Blaise Pascal, F-67 000 Strasbourg, France; e-mail: daniel@quantix.u-strasbg.fr*

Received September 5, 2002
Accepted November 22, 2002

Dedicated to Professors Petr Čársky, Ivan Hubač and Miroslav Urban on the occasion of their 60th birthdays.

This contribution presents the results of the TD-DFT and CASSCF/CASPT2 calculations on $[W(CO)_4(MeDAB)]$ (MeDAB = *N,N′*-dimethyl-1,4-diazabutadiene), $[W(CO)_4(en)]$ (en = ethylenediamine), $[W(CO)_5(py)]$ (py = pyridine) and $[W(CO)_5(CNpy)]$ (CNpy = 4-cyanopyridine) complexes. Contrary to the textbook interpretation, calculations on the model complex $[W(CO)_4(MeDAB)]$ and $[W(CO)_5(CNpy)]$ show that the lowest W→MeDAB and W→CNpy MLCT excited states are immediately followed in energy by several W→CO MLCT states, instead of ligand-field (LF) states. The lowest-lying excited states of $[W(CO)_4(en)]$ system were characterized as $W(CO_{eq})_2 \rightarrow CO_{ax}$ CT excitations, which involve a remarkable electron density redistribution between axial and equatorial CO ligands. $[W(CO)_5(py)]$ possesses closely-lying W→CO and W→py MLCT excited states. The calculated energies of these states are sensitive to the computational methodology used and can be easily influenced by a substitution effect. The calculated shifts of $[W(CO)_4(en)]$ stretching CO frequencies due to excitation are in agreement with picosecond time-resolved infrared spectroscopy experiments and confirm the occurrence of low-lying M→CO MLCT transitions. No LF electronic transitions were found for either of the complexes studied in the region up to 4 eV.

Keywords: Time dependent density functional; Complete active space SCF; UV-VIS spectroscopy; Time-resolved infrared spectroscopy; Tungsten complexes; Charge transfer; Excited states; DFT calculations; *Ab initio.*

The low-lying excited states responsible for the absorption in the visible and near-UV spectral regions and the photophysical and photochemical behavior of mixed-ligand transition metal (Cr, Mo or W in d^6 configuration) carbonyls $[M(CO)_5L]$ (L = pyridine derivative or piperidine) and $[M(CO)_4(\alpha\text{-diimine})]$ (α-diimine = 2,2′-bipyridine, 1,10-phenanthroline, pyridine-2-carbaldehydes or bis(alkylimino)ethenes R–N=CH–CH=N–R, abbreviated R-DAB) were usually interpreted in terms of interplaying low-lying metal to ligand charge transfer (MLCT) and ligand-field (LF) electronic transitions[1]. It was assumed that the intense visible absorption band and the following weak feature in the near-UV region of $[W(CO)_4(R\text{-DAB})]$ originate in $5d(W)\rightarrow\pi^*(DAB)$ MLCT and LF transitions, respectively. The lowest-lying transition within $[M(CO)_4(en)]$ was interpreted as LF because the ethylenediamine (en) ligand lacks any low-lying π^* orbitals into which a MLCT transition can be directed. According to recent theoretical calculations, the interpretation based on the assignment of weak spectral features to LF transitions is not necessarily correct: DFT [2–4] and CASSCF/CASPT2 [5] calculations on $M(CO)_6$ (M = Cr, Mo, W) and $Ni(CO)_4$ assigned the lowest states as M→CO MLCT, while LF states were calculated at much higher energies. Also TD-DFT calculations[6,7] of $[W(CO)_4(phen)]$ (phen = 1,10-phenanthroline) and $[W(CO)_4(tmp)]$ (tmp = 3,4,7,8-tetramethyl-1,10-phenanthroline) and CASSCF/CASPT2 calculations[8–10] of $[Cr(CO)_4(bpy)]$ of (bpy = 2,2′-bipyridine), have shown that lowest W→diimine MLCT excited states are immediately followed in energy by several M→CO MLCT states. LF states were again calculated to lie much higher in energy. The *ab initio* calculations[11] of the vibrational frequencies of the model complex $[W(CO)_4(NH_3)]$ in its ground and lowest excited states showed that excitation influences the W–C and C–O bonds. All these results suggest that M→CO MLCT excited states play a very important role in the spectroscopy and photochemistry of mixed-ligand carbonyl complexes.

In order to understand the dependence of the photophysics and photochemistry of these complexes on the ligands L, it is necessary to develop a correct description of electronic transitions in $[M(CO)_4L]$ and $[M(CO)_5L']$ complexes. $[W(CO)_4L]$ (L = en, R-DAB) complexes were experimentally characterized[12] by UV-VIS, resonance Raman and time-resolved IR spectroscopy. DFT calculations were used for description of geometrical parameters and spectral features of $[W(CO)_4L]$ complexes. The present work compares the performance of two different quantum chemical techniques, TD-DFT and CASSCF/CASPT2, in order to get a more detailed theoretical insight into electronic transitions of the complexes and support the spectral assignment. In the CASSCF/CASPT2 method, contrary to TD-DFT, the dy-

namic electronic correlation is added as a perturbation on top of a zero-order multiconfigurational wavefunction. Other goal of this work is to compare the performance of different density functionals BP86 and hybrid B3LYP. The present study also extends the studied series of molecules by two $[W(CO)_5L]$ complexes (L = py, CNpy). It is examined how the type of the coordination sphere and variation of the ligand L influence the character and the order of lowest excited states and, consequently, the photochemical and photophysical behavior. In particular, electronic transitions of all complexes were analyzed and characterized in terms of changes of electron density distribution.

COMPUTATIONAL

The ground-state electronic structures of $[W(CO)_4(en)]$, $[W(CO)_4(MeDAB)]$, $[W(CO)_5(py)]$ and $[W(CO)_5(CNpy)]$ complexes were calculated by density functional theory (DFT) method using the Gaussian 98 program package[13]. Lowest excited states of the closed-shell complexes were calculated by the time-dependent DFT (TD-DFT) method and CASSCF/CASPT2 (MOLCAS program packages[14]). Gaussian 98 was also used to calculate vibrational frequencies at optimized geometries corresponding to the functional and basis set used. The IR spectrum of the $[W(CO)_4(en)]$ excited state was modeled by unrestricted Kohn–Sham calculations for the lowest-lying ^3B triplet state. The electrostatic solvent influence on vibrational frequencies was modeled using the polarizable continuum model[15] (PCM) incorporated into G98.

Within Gaussian 98, the Dunning's polarized valence double ζ basis sets[16] were used for H, C, N and O atoms and the quasirelativistic effective core pseudopotentials and corresponding optimized set of basis functions[17] for W. In these calculations, the hybrid Becke's three-parameter functional with the Lee, Yang and Parr correlation functional (B3LYP)[18] was used (G98/B3LYP). This technique was employed for geometry optimization, calculations of vibrational frequencies and electronic transition energies. The shape of molecular orbitals as well as the accompanying changes in electron-density distribution were determined from these calculations. The changes in electron density on going from the electronic ground state to the excited state, as described by TD-DFT, are given by the differences in Mulliken populations. Comparable calculations were done with the BP86 non-hybrid functional including Becke's gradient correction[19] to the local exchange expression in conjunction with Perdew's gradient correction[20] to the LDA expression (BP86).

CASSCF/CAPT2 calculations used the same basis set as that employed in the G98 DFT calculations. In all cases, the CASSCF active space included the three highest occupied orbitals of a prevailing 5d(W) character and six electrons were correlated. The influence of the active space size was examined for the $[W(CO)_4(en)]$ case, for which total 8 or 16 orbitals were used for correlation. The CASSCF active space contained eleven, nine and nine orbitals for $[W(CO)_4(MeDAB)]$, $[W(CO)_5(py)]$ and $[W(CO)_5(CNpy)]$, respectively. Lowest roots were calculated by a state-averaged procedure. The CASSCF wavefunctions were used as references in subsequent CASPT2 calculations using the multi-state level shift corrected perturbation method[21].

$[W(CO)_4(MeDAB)]$, $[W(CO)_5(py)]$ and $[W(CO)_5(CNpy)]$ complexes were calculated under the C_{2v} symmetry constraint while $[W(CO)_4(en)]$ was approximated as C_2.

EXPERIMENTAL

Both the ground- and excited-state IR spectra of $[W(CO)_4(en)]$ were obtained in a CH_3CN solution. The experimental set-up used to measure the picosecond time-resolved IR spectra has been described in detail elsewhere[22,23]. Briefly, the sample was excited with 400 nm laser pulses of an approximately 250 fs duration and probed, after a specified time-delay, with broad-band IR pulses of a comparable duration which cover a spectral window 150–200 cm^{-1} wide. The experiment provides difference IR spectra, expressed as the spectrum obtained at a selected time delay after excitation minus the spectrum before excitation. Hence, the experimental spectrum contains positive features corresponding to the photoproduced excited state and negative features due to the depleted ground-state population. The latter is a mirror image of the ground-state IR spectrum. A strong overlap of the IR features due to the ground and excited states of $[W(CO)_4(en)]$ complicates the determination of the excited-state spectrum and correction for the bleached ground-state absorption is needed. This was accomplished by a scaled numerical addition of the ground-state spectrum to the time-resolved difference spectrum. The regions 1750–1910 and 1925–2120 cm^{-1} were treated separately since each of them was measured as a single spectral window using the same IR probe-beam. The intensity of the added ground-state spectrum was scaled commensurately to the intensity of the bleached 1865 cm^{-1} peak to obtain the corrected excited-state spectrum in the 1750–1910 cm^{-1} region while the 2004 cm^{-1} ground-state band was used in the 1925–2120 cm^{-1} range. Excited-state spectra determined from the time-resolved spectra measured at 8 and 50 ps after excitation are essentially identical. Both these time delays are sufficiently long to preclude any effects of early vibrational relaxation that occurs between 1 and 5 ps [12].

RESULTS AND DISCUSSIONS

The molecular structures of all complexes were optimized by G98/B3LYP DFT calculations. The optimized structures were used in following TD-DFT and CASPT2 calculations. $[W(CO)_5L]$ complexes (L = py, CNpy) exhibit two

energy minima: first for the configuration in which the pyridine plane is coincident with one C_{eq}–W–C_{eq} moiety (Fig. 1), the second for the pyridine plane bisecting the C_{eq}–W–C_{ax} angle. Energies of both configurations are almost identical, while a small rotation barrier is found between the energy minima. The configuration with the py plane coincident with a C_{eq}–W–C_{eq} moiety was used within this study for both $[W(CO)_5L]$ complexes. The influence of py rotation on ground- and excited-state properties will be published elsewhere[24].

Electronic Transitions of [W(CO)$_4$(en)]

Table I compares the electronic transitions of $[W(CO)_4(en)]$ calculated using TD-DFT (BP86 and B3LYP functional) and CASPT2 with the experimental spectra. The shoulder at 2.71 eV is attributed to the lowest spin-forbidden $a^1A \rightarrow a^3B$ transition and the main absorption band at 3.12 eV to the $a^1A \rightarrow a^1B$ transition. These transitions originate in excitation from the metal-based HOMO (27a) into the CO-localized LUMO (26b) (see Fig. 2 for the CASSCF/CASPT2 calculated shapes of these frontier orbitals). Both methods also indicate that a weak $a^1A \rightarrow b^1A$ transition lies close in energy to the main $a^1A \rightarrow a^1B$ transition. CASPT2 calculations based on a smaller active space reverse the order of these two transitions. Table II shows the electron density redistribution within the $[W(CO)_4(en)]$ molecule upon its $a^1A \rightarrow a^1B$ and $a^1A \rightarrow b^1A$ transitions calculated using several theoretical approaches. Inspection of the corresponding density differences indicates that both these transitions can be described as a charge transfer from a $W(CO_{eq})_2$ fragment formed by the W atom and the two equatorial CO lig-

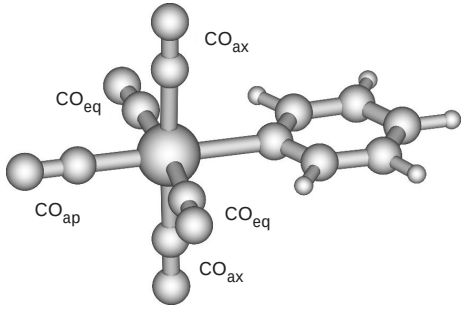

FIG. 1
Molecular structure of $[W(CO)_5(py)]$ optimized by G98/B3LYP DFT calculations. The pyridine plane is coincident with one C_{eq}–W–C_{eq} moiety

ands to the axial CO ligands. The notation equatorial (eq) and axial (ax) stands for the CO ligands lying in and perpendicular to the NWN plane, respectively. This finding contradicts the previous interpretation assigning the 3.12 eV absorption band to a LF transition[25–28]. Both CASPT2 and TD-DFT afford a qualitatively similar description of the electron density redistribution, the TD-DFT calculation showing larger charge transfer among individual subsystems. Enlarging the CASSCF active space does not change the qualitative description of the excitation although a smaller electron-density decrease on the W atom was obtained using a larger active space.

TABLE I
Selected calculated low-lying excitation energies (in eV) for $[W(CO)_4(en)]$ with oscillator strength larger than 0.001. Oscillator strengths and extinction coefficients in parenthesis. Experimental data obtained in CH_3CN

State	Character	TD-DFT (B3LYP)	TD-DFT (BP86)	CASPT2	Experiment[12]
a^3B	$W(CO_{eq})_2 \rightarrow CO_{ax}$	2.35 (–)	2.28 (–)	–	2.71 (190)
a^1B	$W(CO_{eq})_2 \rightarrow CO_{ax}$	2.62 (0.011)	2.47 (0.007)	2.69 (0.025)	
b^1A	$W(CO_{eq})_2 \rightarrow CO_{ax}$	2.75 (0.001)	2.52 (0.001)	2.86 (0.001)	3.12 (1400)
c^1B	MLCT–W→CO	3.63 (0.032)	3.55 (0.054)	3.95 (0.059)	
d^1B	MLCT–W→CO	4.15 (0.002)	3.99 (0.002)	3.98 (0.003)	4.12 (8320)

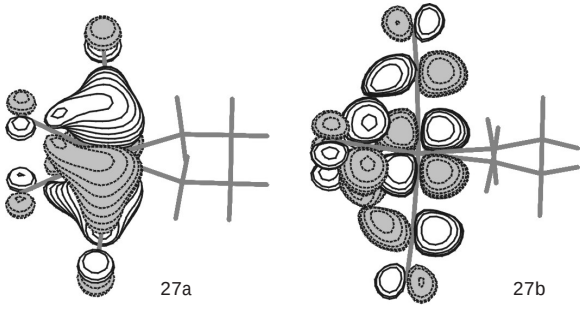

FIG. 2
Shapes of the 27a and 26b orbitals of $[W(CO)_4(en)]$ calculated by CASSCF/CASPT2

Comparison of the values obtained with the B3LYP and BP86 functionals indicates that the change of the density functional does not influence the qualitative assignment. Similar results were obtained with the asymptotically correct SAOP functional[12].

The principal $a^1A \rightarrow a^1B$ transition was calculated by TD-DFT to arise predominantly (97%) from 27a→26b excitation. Inclusion of the dynamic correlation does not change this picture substantially since the CASPT2 calculation has shown the ground-state configuration $(26a)^{1.91}(25b)^{1.89}(27a)^{1.88}(26b)^{0.07}(28a)^{0.07}$ and 78% contribution of the 27a→26b excitation to the lowest excited state. This result enables us to model the lowest excited state by a single-determinantal triplet electronic configuration $(27a)^1(26b)^1$. The geometry optimization of this state and comparison of the calculated frequencies of CO stretching vibrations, ν(CO), with the excited-state IR spectrum helps to verify the proposed assignment of the lowest excited state as a^3B. For this purpose, the previously measured picosecond time-resolved difference IR spectrum[12] was analyzed to obtain a pure spectrum of the lowest triplet excited state (see Experimental). The calculated ν(CO) frequencies (B3LYP calculation with PCM correction in CH_3CN cavity) together with the experimental IR band half-widths were used to model the theoretical IR spectra. For description of ν(CO) vibrations the C_{2v} symmetry of $W(CO)_4$ fragment is used: A_1^2 (in-phase, predomi-

TABLE II
CASPT2- and TD-DFT-calculated changes in Mulliken populations during the lowest allowed transitions of the $[W(CO)_4(en)]$ complex. Values of $(CO)_{ax}$ and $(CO)_{eq}$ regard to the population changes on individual axial and equatorial CO ligands

Transition	Method	W	$(CO)_{ax}$	$(CO)_{eq}$	en
$a^1A \rightarrow a^1B$	CASPT2[a]	–0.053	0.117	–0.078	–0.025
	CASPT2[b]	–0.087	0.127	–0.085	0.004
	TD-DFT[c]	–0.248	0.269	–0.172	0.054
	TDDFT[d]	–0.367	0.337	–0.185	0.064
$a^1A \rightarrow b^1B$	CASPT2[a]	–0.118	0.126	–0.067	0.000
	CASPT2[b]	–0.154	0.125	–0.048	0.001
	TD-DFT[c]	–0.011	0.222	–0.188	–0.057
	TD-DFT[d]	–0.314	0.290	–0.190	0.112

[a] CASPT2, large active space (6 electrons in 16 active orbitals). [b] CASPT2, small active space (6 electrons in 8 active orbitals). [c] TD-DFT (B3LYP). [d] TD-DFT (BP86).

nantly axial CO stretch), B_1 (antisymmetric axial CO stretch), A_1^1 (out-of-phase, predominantly equatorial CO stretch) and B_2 (antisymmetric equatorial CO stretch) (indicated in Figs 3 and 4). The comparison of Figs 3 and 4 shows that the theoretical ground- and excited-state spectra well reproduce the ground-state ν(CO) frequencies and their shifts upon the $a^1A \rightarrow a^3B$ transition, as well as the corresponding patterns of IR band intensities. The shift of the higher A_1^2 vibration upon excitation (–20 cm^{-1}) is slightly underestimated. Importantly, the calculations predict the order of the wavenumbers of the three lowest ν(CO) vibrations $A_1^1 < B_2 < B_1$ in agreement with the experiment. The obtained good correspondence between the experimental and calculated ν(CO) frequencies of $[W(CO)_4(en)]$

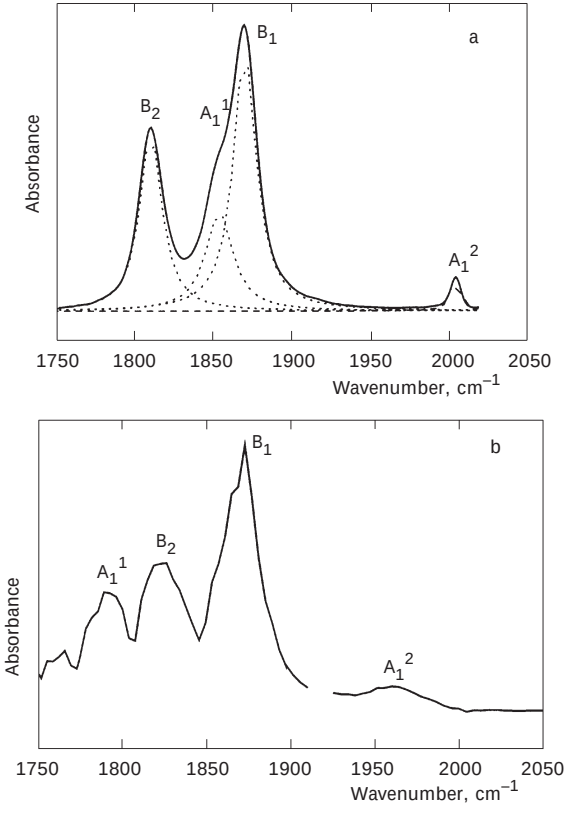

FIG. 3

The exprerimental ground state spectrum of $[W(CO)_4(en)]$ in CH_3CN (a) and 50 ps TRIR spectrum of $[W(CO)_4(en)]$ in CH_3CN corrected for bleached ground-state absorption (b). Dotted line indicates the individual Lorenzians of deconvoluted ground state spectrum

in its ground and the lowest a^3B excited state confirms our theoretical conclusions about the character of the lowest excited state and the changes of W–CO bonding and electron density distribution upon electronic excitation (*vide supra*).

The strong UV absorption band at 4.12 eV was also calculated to belong to a highly delocalized transition which includes an important W→CO contribution.

In conclusion, it was found that both TD-DFT and CASSCF/CASPT2 reproduce well the absorption spectrum of $[W(CO)_4(en)]$. It should be noted that neither of these techniques found any predominantly LF transition in the investigated energy region up to 4.12 eV.

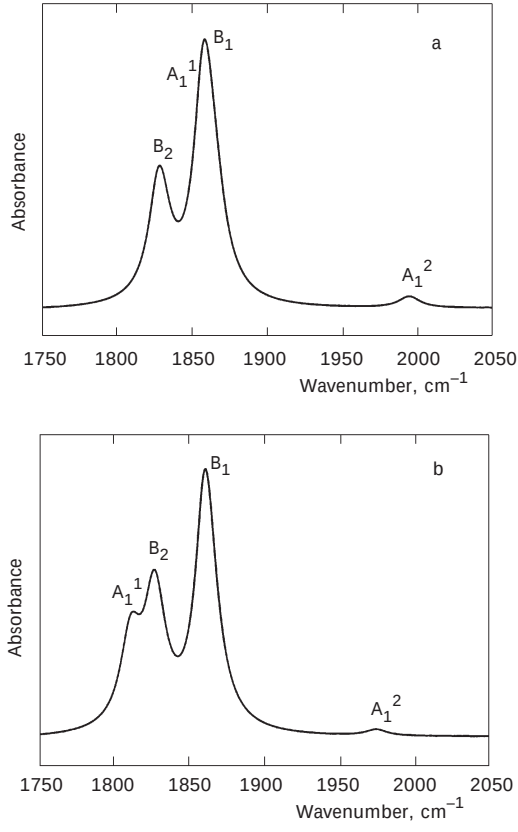

FIG. 4

Simulated ground (a) and excited state (b) IR spectra of $[W(CO)_4(en)]$ from B3LYP calculation with PCM correction in CH_3CN cavity

Electronic Transitions of [W(CO)$_4$(MeDAB)]

The lowest allowed electronic transition $a^1A_1 \rightarrow b^1A_1$ of the model [W(CO)$_4$(MeDAB)] was calculated by CASPT2 at 2.29 eV (see Table III for the summary of the calculated and experimental spectra, well reproducing the intense 2.33 eV absorption band of [W(CO)$_4$(*t*-Bu-DAB)]). The TD-DFT (B3LYP) technique calculated this transition at a somewhat higher energy of 2.65 eV. This transition corresponds predominantly to HOMO-2 ($22b_1$)→LUMO ($23b_1$), excitation. The weak $a^1A_1 \rightarrow a^1B_2$ transition (1.54 eV CASPT2, 1.77 eV TD-DFT) gives rise to the low-energy shoulder observed in the spectra at *ca* 1.89 eV. The calculated redistribution of electron density upon $a^1A_1 \rightarrow b^1A_1$ and $a^1A_1 \rightarrow a^1B_2$ transitions (Table IV) clearly demonstrates the W→DAB MLCT character of these transitions, in agreement with the previous empirical assignment[29–32]. It should be noted that the electron density decreases significantly not only at the W atom but also at the CO ligands. These transitions should thus be more correctly viewed as W(CO)$_4$→DAB CT, involving the whole W(CO)$_4$ fragment. This conclusion is in agreement with our previous study[9] of [Cr(CO)$_4$(bpy)]. Data in Table IV also show that the decrease in the electron density on the CO ligands calculated by CASPT2 is much larger than that obtained by TD-DFT. This is at the expense of the depopulation of W orbitals, which was calculated much larger by TD-DFT than using CASSCF/CASPT2. The W→DAB MLCT

TABLE III
Selected calculated low-lying singlet excitation energies (in eV) for [W(CO)$_4$(MeDAB)] with oscillator strength larger than 0.001. Oscillator strengths and extinction coefficients in parenthesis

State	Character	TD-DFT (B3LYP)	TD-DFT (BP86)	CASPT2	Experiment[a]
a^1B_2	MLCT-W→MeDAB HOMO→LUMO	1.77 (0.001)	1.68 (0.001)	1.54 (0.000)	1.89 (sh)
b^1A_1	MLCT-W→MeDAB HOMO-2→LUMO	2.64 (0.175)	2.68 (0.145)	2.29 (0.382)	2.33 (6000)
b^1B_2	MLCT-W→CO	3.04 (0.008)	2.78 (0.004)	2.90 (0.010)	
c^1A_1	MLCT-W→CO	3.40 (0.001)	3.06 (0.004)	3.69 (0.002)	3.30 (1040)
b^1B_1	MLCT-W→CO	3.41 (0.007)	3.37 (0.007)	3.10 (0.013)	

[a] Experimental data obtained in CH_2Cl_2, strong absorption above 3.75 eV was not studied in detail[12].

transitions are followed in energy by three transitions $a^1A_1 \rightarrow b^1B_2$, $a^1A_1 \rightarrow c^1A_1$ and $a^1A_1 \rightarrow b^1B_1$ which give rise to the relatively weak absorption band at 3.30 eV. The calculated changes of electron density distribution (Table IV) shows that the $a^1A_1 \rightarrow b^1B_2$ transition, calculated at 2.90 eV by CASPT2 and 3.04 eV by TD-DFT (B3LYP) has a $W(CO_{eq})_2 \rightarrow CO_{ax}$ CT character. Transitions directed to the c^1A_1 and b^1B_1 states lie at slightly higher energies and both have a mixed $W \rightarrow CO_{ax}$ and $W(CO_{eq})_2 \rightarrow CO_{ax}$ character. The $a^1A_1 \rightarrow b^1B_2$, $a^1A_1 \rightarrow c^1A_1$ and $a^1A_1 \rightarrow b^1B_1$ transitions are analogous to the lowest three transitions of $[W(CO)_4(en)]$ (*vide supra*). It follows that the weak absorption band observed in the experimental spectrum of $[W(CO)_4$(*t*-Bu-DAB)] and analogous complexes at *ca* 3.30 eV actually belongs to W→CO CT transitions. This conclusion contradicts the previous empirical assignment of this band as LF. In fact, no genuine LF transitions were found by CASPT2 and TD-DFT for $[W(CO)_4$(MeDAB)] at energies up to 4 eV.

Electronic Transitions of $[W(CO)_4(py)]$

Table V shows the TD-DFT and CASPT2 calculated electronic transitions of $[W(CO)_5(py)]$, compared with the experimental spectra. The TD-DFT method using the B3LYP functional assigns the most intense transition $a^1A_1 \rightarrow b^1A_1$ as excitation from the predominantly W(5d) $12b_1$ molecular orbital into the $13b_1$ π* py molecular orbital. The calculated value of 3.13 eV well reproduces the experimental transition energy (3.25 eV). TD-DFT with non-hybrid BP86 functional underestimated (calculated at 2.69 eV) and

TABLE IV

CASPT2- and TD-DFT-calculated changes in Mulliken populations during the lowest allowed transitions of the $[W(CO)_4$(MeDAB)] complex. Values of $(CO)_{ax}$ and $(CO)_{eq}$ regard to the population changes on individual axial and equatorial CO ligands

Transition	Method	W	$(CO)_{ax}$	$(CO)_{eq}$	MeDAB
$a^1A_1 \rightarrow a^1B_2$	CASPT2[a]	–0.236	–0.057	–0.056	0.461
	TD-DFT[b]	–0.468	–0.047	–0.055	0.673
$a^1A_1 \rightarrow b^1A_1$	CASPT2[a]	–0.177	–0.013	–0.024	0.247
	TD-DFT[b]	–0.271	0.002	–0.039	0.346
$a^1A_1 \rightarrow b^1B_2$	CASPT2[a]	–0.162	0.229	–0.170	0.044
	TD-DFT[b]	–0.439	0.372	–0.166	0.026

[a] CASPT2 (6 electrons in 16 active orbitals). [b] TD-DFT (B3LYP).

CASPT2 overestimates (calculated at 3.63 eV) the excitation energy of this transition. As follows from Table VI, the $a^1A_1 \rightarrow b^1A_1$ transition can be characterized as MLCT from the $W(CO)_5$ fragment into the py ligand, since both TD-DFT and CASPT2 methods predict that approximately 0.8 e^- is transferred into the pyridine π^* system. The lowest-lying transition observed at 2.81 eV is assigned as the $a^1A_1 \rightarrow a^1B_1$ transition from a metal-centered molecular orbital into π^* orbitals of the equatorial CO ligands, accompanied by the charge reorganization among the remaining CO ligands. This transition is calculated at 3.02 and 3.4 eV by TD-DFT/B3LYP and CASPT2 methods, respectively. TD-DFT calculation with the BP86 functional reverses the order of $a^1A_1 \rightarrow a^1A_1$ and $a^1A_1 \rightarrow a^1B_1$ transitions and underestimates the calculated energies. The excited states calculated at higher energies with low oscillator strengths have a mixed W→CO character.

TABLE V
Selected calculated low-lying singlet excitation energies (in eV) for $[W(CO)_5(py)]$ with oscillator strength larger than 0.001. Oscillator strengths and extinction coefficients in parenthesis

State	Character	TD-DFT (B3LYP)	TD-DFT (BP86)	CASPT2	Experiment
a^1B_1	MLCT-W→CO	3.02 (0.014)	2.95 (0.010)	3.40 (0.034)	2.81 (615)
b^1A_1	MLCT-W→py	3.13 (0.135)	2.69 (0.124)	3.63 (0.232)	3.25 (7480)
a^1B_2	MLCT-W→CO	3.14 (0.013)	3.06 (0.011)	3.47 (0.054)	3.49 (6800)
c^1A_1	MLCT-W→CO	3.64 (0.019)	3.47 (0.004)	3.86 (0.014)	3.71 (w)

TABLE VI
TD-DFT- and CASPT2-calculated changes in Mulliken populations during the lowest allowed transitions of the $[W(CO)_5(py)]$. Values of $(CO)_{ax}$ and $(CO)_{eq}$ regard to the population changes on individual axial and equatorial CO ligands

State	Method	W	$(CO)_{ax}$	$(CO)_{eq}$	$(CO)_{ap}$	py
a^1B_1	CASPT2[a]	–0.115	–0.059	0.168	–0.088	–0.014
	TD-DFT[b]	–0.350	0.013	0.243	–0.149	–0.015
b^1A_1	CASPT2[a]	–0.302	–0.081	–0.147	–0.048	0.808
	TD-DFT[b]	–0.527	–0.103	0.001	–0.109	0.839

[a] CASPT2 (6 electrons in 9 active orbitals). [b] B3LYP.

Electronic Transitions of $[W(CO)_4(CNpy)]$

The calculated and experimental transition energies and oscillator strengths of $[W(CO)_5(CNpy)]$ are summarized in Table VII. Both TD-DFT and CASPT2 methods assign the lowest-lying intense transition of $[W(CO)_5(CNpy)]$ as $a^1A_1 \rightarrow b^1A_1$, similar to the first intense transition of $[W(CO)_5(py)]$. This transition is characterized as MLCT from the predominantly W(5d) $13b_1$ molecular orbital into the $14b_1$ π^* CNpy molecular orbital. It also involves depopulation of CO π^* orbitals and reorganization of the electron density among the CO ligands (Table VIII). Calculations correctly reproduce the substituent effect of the CN group, which shifts this transition to lower energy. The absolute value of the substituent shift is overestimated by both

TABLE VII
Selected calculated low-lying singlet excitation energies (in eV) for $[W(CO)_5(CNpy)]$ with oscillator strength larger than 0.001. Oscillator strengths and extinction coefficients in parenthesis

State	Character	TD-DFT (B3LYP)	TD-DFT (BP86)	CASPT2	Experiment[a]
a^1A_1	MLCT-W→CNpy	2.50 (0.208)	2.14 (0.223)	2.84 (0.179)	2.72 (7060)
a^1B_1	MLCT-W→CO	3.07 (0.012)	3.13 (0.015)	3.16 (0.042)	3.07 (5530)
a^1B_2	MLCT-W→CO	3.14 (0.012)	3.18 (0.009)	3.21 (0.033)	3.34 (sh)

[a] Experimental values taken from[33].

TABLE VIII
TD-DFT- and CASPT2-calculated changes in Mulliken populations during the lowest allowed transitions of the $[W(CO)_5(CNpy)]$. Values of $(CO)_{ax}$ and $(CO)_{eq}$ regard to the population changes on individual axial and equatorial CO ligands

L	State	Method	W	$(CO)_{ax}$	$(CO)_{eq}$	$(CO)_{ap}$	CNpy
CNpy	b^1A_1	CASPT2[a]	–0.323	–0.071	–0.061	–0.053	0.640
		TD-DFT[b]	–0.513	–0.114	0.026	–0.106	0.794
CNpy	a^1B_1	CASPT2[a]	–0.119	–0.060	0.188	–0.124	–0.012
		TD-DFT[b]	–0.363	0.002	0.264	–0.145	–0.023

[a] CASPT2 (6 electrons in 9 active orbitals). [b] B3LYP.

methods. The experimental transition energy is reasonably well reproduced by the CASPT2 method, while TD-DFT (B3LYP and BP86) locates the calculated energies at lower values (Table VII).

Tables VII and VIII also show that the relative order of the $a^1A_1 \rightarrow b^1A_1$ and $a^1A_1 \rightarrow a^1B_1$ transitions is interchanged by the CN substitution. W→CO transitions lie at higher energies than the main MLCT transition into π* CNpy in $[W(CO)_5(CNpy)]$ while the W→CO CT transitions are the lowest in $[W(CO)_5(py)]$. Analogously to unsubstituted $[W(CO)_5(py)]$, the $a^1A_1 \rightarrow a^1B_1$ transition involves the charge transfer prevailingly from the metal to π* orbitals of the equatorial CO ligands.

CONCLUSIONS

The electronic spectra of $[W(CO)_4(en)]$, $[W(CO)_4(MeDAB)]$, $[W(CO)_5(py)]$ and $[W(CO)_5(CNpy)]$ complexes were reinterpreted on the basis of TD-DFT and CASSCF/CASPT2 calculations. In contrast to the standard textbook assignment, the lowest excited states were identified to be either W→π*(L) or W→π*(CO) MLCT, depending on the type of the hetero-ligand. No pure LF (dd) transitions occur in the visible or near-UV spectral regions. It has been shown that W→CO MLCT states instead of LF are responsible for spectral and photophysical behavior induced by visible or near-UV irradiation.

The lowest-lying excited states of $[W(CO)_4(en)]$ were identified as $W(CO_{eq})_2 \rightarrow CO_{ax}$ CT states, followed by other W→CO states. According to the TD-DFT results, and confirmed by CASPT2 calculation, the lowest excited state of $[W(CO)_4(en)]$ is sufficiently pure to be modeled by a single determinantal triplet ^3B wave function. The vibrational analysis based on the lowest one-determinantal state enabled us to interpret the time-resolved IR experiment and verify the theoretical conclusions regarding the character of the lowest excited state.

TD-DFT as well as CASPT2 calculations identified close-lying W→π*(CO) and W→π*(pyridine) MLCT states in $[W(CO)_5(py)]$. The calculated relative position of these states is sensitive to the computational details (density functional used, CASSCF active space) and the orientation of the pyridine ligand. The relative order of these states can be easily interchanged by the variation of the substituent on the pyridine ligand. In agreement with the experiment, both methods identify the lowest weak absorption feature as a transition into a W→π*(CO) MLCT state, followed in energy by a W→π*(pyridine) MLCT transition which is manifested by a strong MLCT absorption band. In $[W(CO)_5(CNpy)]$ complex the order of these states is reversed.

No genuine LF transitions were calculated for either of the complexes investigated in the energy range up to 4 eV. It follows that LF transitions and excited states play a much smaller role in the spectroscopy, photophysics and photochemistry of carbonyl complexes than is usually assumed.

Funding of the Ministry of Education, Youth and Sports of the Czech Republic (grant OC.D14.20), COST Action D14 and EPSRC (UK) is gratefully acknowledged. P. Matousek (CLRC, Rutherford Appleton Laboratory) and I. R. Farrell (QMUL, now RSC) are thanked gratefully for their help with the measurements of the picosecond time-resolved IR spectra.

REFERENCES

1. Geoffroy G. L., Wrighton M. S.: *Organometallic Photochemistry*. Academic Press, New York 1979.
2. Pollak C., Rosa A., Baerends E. J.: *J. Am. Chem. Soc.* **1997**, *119*, 7324.
3. Rosa A., Baerends E. J., van Gisbergen S. J. A., van Lenthe E., Groeneveld J. A., Snijders J. G.: *J. Am. Chem. Soc.* **1999**, *121*, 10356.
4. Baerends E. J., Rosa A.: *Coord. Chem. Rev.* **1998**, *177*, 97.
5. Pierloot K., Tsokos E., Vanquickenborne L. G.: *J. Phys. Chem.* **1996**, *100*, 16545.
6. Farrell I. R., Hartl F., Záliš S., Mahabiersing T., Vlcek A., Jr.: *J. Chem. Soc., Dalton Trans.* **2000**, 4323.
7. Farrell I. R., van Slageren J., Záliš S., Vlcek A., Jr.: *Inorg. Chim. Acta* **2001**, *315*, 44.
8. Guillaumont D., Daniel C., Vlcek A., Jr.: *Inorg. Chem.* **1997**, *36*, 1684.
9. Záliš S., Daniel C., Vlcek A., Jr.: *J. Chem. Soc., Dalton Trans.* **1999**, 3081.
10. Guillaumont D., Daniel C., Vlček A., Jr.: *J. Phys. Chem. A* **2001**, *105*, 1107.
11. Zaric S., Couty M., Hall M. B.: *J. Am. Chem. Soc.* **1997**, *119*, 2885.
12. Záliš S., Farrell I. R., Vlček A., Jr.: *J. Am. Chem. Soc.*, in press.
13. Frisch M. J., Trucks G. W., Schlegel H. B., Scuseria G. E., Robb M. A., Cheeseman J. R., Zakrzewski V. G., Montgomery J. A., Jr., Stratmann R. E., Burant J. C., Dapprich S., Millam J. M., Daniels A. D., Kudin K. N., Strain M. C., Farkas O., Tomasi J., Barone V., Cossi M., Cammi R., Mennucci B., Pomelli C., Adamo C., Clifford S., Ochterski J., Petersson G. A., Ayala P. Y., Cui Q., Morokuma K., Malick D. K., Rabuck A. D., Raghavachari K., Foresman J. B., Cioslowski J., Ortiz J. V., Baboul A. G., Stefanov B. B., Liu G., Liashenko A., Piskorz P., Komaromi I., Gomperts R., Martin R. L., Fox D. J., Keith T., Al-Laham M. A., Peng C. Y., Nanayakkara A., Gonzalez C., Challacombe M., Gill P. M. W., Johnson B., Chen W., Wong M. W., Andres J. L., Gonzalez C., Head-Gordon M., Replogle E. S., Pople J. A.: *Gaussian 98*, Revision A.7. Gaussian. Inc., Pittsburgh (PA) 1998.
14. Andersson K., Blomberg M. R. A., Fülscher M. P., Karlström G., Lindh R., Malmqvist P.-Å., Neogrady P., Olsen J., Roos B. O., Sadlej A. J., Schütz M., Seijo L., Serrano-Andrés L., Siegbahn P. E. M., Widmark P.-O.: *MOLCAS*, Version 4.1. Lund University, Lund 1997.
15. Amovilli C., Barone V., Cammi R., Cances E., Cossi M., Mennucci B., Pomelli C. S., Tomasi J.: *Adv. Quantum Chem.* **1999**, *32*, 227.
16. Woon D. E., Dunning T. H., Jr.: *J. Chem. Phys.* **1993**, *98*, 1358.

17. Andrae D., Häussermann U., Dolg M., Stoll H., Preuss H.: *Theor. Chim. Acta* **1990**, *77*, 123.
18. Stephens P. J., Devlin F. J., Cabalowski C. F., Frisch M. J.: *J. Phys. Chem.* **1994**, *98*, 11623.
19. Becke A. D.: *Phys. Rev. A: At., Mol., Opt. Phys.* **1988**, *38*, 3098.
20. Perdew J. P.: *Phys. Rev. A: At., Mol., Opt. Phys.* **1986**, *33*, 8822.
21. Roos B. O., Andersson K., Fülscher M. P., Serrano-Andrés L., Pierloot K., Merchán M., Molina V.: *J. Mol. Struct. (THEOCHEM)* **1996**, *388*, 257.
22. Towrie M., Grills D. C., Matousek P., Parker A. W., George M. W.: *Appl. Spectrosc.*, in press.
23. Vlček A., Jr., Farrell I. R., Liard D. J., Matousek P., Towrie M., Parker A. W., Grills D. C., George M. W.: *J. Chem. Soc., Dalton Trans.* **2002**, 701.
24. Záliš S., Kotrba T., Daniel C., Vlček, A., Jr.: Unpublished results.
25. Saito H., Fujita J., Saito K.: *Bull. Chem. Soc. Jpn.* **1968**, *41*, 359.
26. Wrighton M. S., Morse D. L.: *J. Organomet. Chem.* **1975**, *97*, 405.
27. Rawlins K. A., Lees A. J.: *Inorg. Chem.* **1989**, *28*, 2154.
28. Panesar R. S., Dunwoody N., Lees A. J.: *Inorg. Chem.* **1998**, *37*, 1648.
29. Stufkens D. J.: *Coord. Chem. Rev.* **1990**, *104*, 39.
30. Vlček A., Jr.: *Coord. Chem. Rev.* **2002**, *230*, 225.
31. Balk R. W., Snoeck T., Stufkens D. J., Oskam A.: *Inorg. Chem.* **1980**, *19*, 3015.
32. Staal L. H., Stufkens D. J., Oskam A.: *Inorg. Chim. Acta* **1978**, *26*, 255.
33. Rawlins K. A., Lees A. J., Adamson A. W.: *Inorg. Chem.* **1990**, *29*, 3866.